

Evaluation of Bibb Graves Bridge Arch in Wetumpka, Alabama

Petrographic Evaluation and Recommendations

ASR Development and Deployment Program
Field Application and Demonstration Projects



U.S. Department of Transportation
Federal Highway Administration

Technical Report Documentation Page

1. Report No. FHWA-HIF-13-063		2. Government Accession No.		3. Recipient's Catalog No.	
4. Title and Subtitle Evaluation of Bibb Graves Bridge Arch in Wetumpka, Alabama: Petrographic Evaluation and Recommendations				5. Report Date June 2010	
				6. Performing Organization Code	
7. Author(s) B. Fournier, M.D.A. Thomas, and K.J. Folliard				8. Performing Organization Report No.	
9. Performing Organization Name and Address The Transtec Group, Inc. 6111 Balcones Drive Austin, TX 78731				10. Work Unit No.	
				11. Contract or Grant No. DTFH61-06-D-00035	
12. Sponsoring Agency Name and Address Office of Pavement Technology Federal Highway Administration 1200 New Jersey Avenue, SE Washington, DC 20590				13. Type of Report and Period Covered	
				14. Sponsoring Agency Code	
15. Supplementary Notes Contracting Officer's Representative (COR): Gina Ahlstrom, HIAP-10					
16. Abstract This report presents the findings of the petrographic examination of concrete cores extracted from two arches of the Bibb Graves Bridge in Wetumpka, Alabama. The evaluation mainly consisted of the Damage Rating Index (DRI), a method that provides a semiquantitative assessment of the damage in concrete based on a count of petrographic features of deterioration generally associated with alkali-silica reaction (ASR).					
17. Key Words Alkali-silica reactivity, reactive aggregates, petrography, evaluation, DRI, concrete, cores, micrograph, deterioration, ettringite			18. Distribution Statement No restrictions. This document is available to the public through the National Technical Information Service, Springfield, VA 22161.		
9. Security Classif. (of this report)	20. Security Classif. (of this page)	21. No of Pages 30		22. Price	

TABLE OF CONTENTS

1	Introduction	3
2	Field Work - Extraction of Cores	3
3	Laboratory Testing of Cores.....	3
3.1	Damage Rating Index (DRI)	3
4	Results of the Petrographic Examination.....	4
4.1	Core 2A-South	4
4.2	Core 2A-North	5
4.3	Core 2B-South	8
4.3	Core 2B-North	8
5	Conclusion - Summary of Findings.....	9
6	Recommendations	9
7	References.....	10
	Appendix A.....	11
	Appendix B	14

LIST OF FIGURES

Figure 1. Polished concrete sections from the Gibb Graves Bridge, Wetumpka, Alabama.	7
Figure 2. Results of the Damage Rating Index (DRI) for the Alabama cores	8

LIST OF TABLES

Table 1. Cores provided for petrographic examination (ALDOT 2010)	3
Table 2. Petrographic Features and Weighing Factors for the DRI (Grattan-Bellew and Mitchell 2006)	4
Table 3. Summary of the petrographic observations on the cores from Alabama (Gibb Graves Bridge)	4

1 Introduction

This report presents the findings of the petrographic examination of concrete cores extracted from two arches of the Bibb Graves Bridge (AL Route 111 over Coosa River) in Wetumpka, Alabama. The evaluation mainly consisted of the Damage Rating Index (DRI), a method that provides a semi-quantitative assessment of the damage in concrete based on a count of petrographic features of deterioration generally associated with alkali-silica reaction (ASR).

2 Field Work - Extraction of Cores

Coring was conducted by ALDOT in January 2010. Cores were extracted from the arches no. 4 and 5 of the bridge, as indicated in Table 1 and illustrated in the Appendix A.

Table 1. Cores provided for petrographic examination (ALDOT 2010)

Core number	Location	Condition
2A-South	South arch # 5; East side of arch	Core in 3 sections
2A-North	North arch # 5; East side of arch	Core in 2 sections
2B-South	South arch # 4; West side of arch	Core in 1 section
2B-North	North arch # 4; West side of arch	Core in 1 section

3 Laboratory Testing of Cores

The concrete cores were sent to Dr. Benoit Fournier at Laval University, Québec, Canada in February 2010. The four cores were first cut in two axially and polished, then examined under the stereomicroscope to determine the Damage Rating Index (DRI).

3.1 Damage Rating Index (DRI)

Grattan-Bellew (1992) and Dunbar and Grattan-Bellew (1995) described a method to evaluate the condition of concrete by counting the number of typical petrographic features of ASR on polished concrete sections (18x magnification) (Table 2). A grid is drawn on the polished concrete section, which includes a minimum of 150 grid squares, 1 cm by 1 cm in size. The *Damage Rating Index* represents the normalized value (to 100 cm²) of the presence of these features after the count of their abundance over the surface examined has been multiplied by weighing factors representing their relative importance in the overall deterioration process (Table 2).

Table 2. Petrographic Features and Weighing Factors for the DRI (Grattan-Bellew and Mitchell 2006)

Petrographic feature	Abbreviation	Weighing factor
Coarse aggregate with cracks	CrCA	x 0.75
Open crack in coarse aggregate	OCrCA	x 4.0
Coarse aggregate with cracks and reaction products	Cr + RPCA	x 2.0
Coarse aggregate debonded	CAD	x 3.0
Reaction rims around aggregate	RR	x 0.5
Cement paste with cracks	CrCP	x 2.0
Cement paste with cracks and reaction products	Cr+RPCP	x 4.0
Air voids lined or filled with reaction products	RPAV	x 0.50

4 Results of the Petrographic Examination

The four polished sections examined as part of this investigation are illustrated in Figure 1, while the results of the DRI are summarized in Figure 2. Table 3 gives a summary of the petrographic observations (in terms of the typical crack width observed in the cement paste of the cores) and a rating of the extent of ASR in the concrete. The detailed results of DRI, including micrographs of the petrographic features in the cores examined, are given in the Appendix B.

There is currently no rating system for the DRI values that correspond to concrete affected to a low, moderate or severe degree by ASR. However, our experience is such that values below 200-250 are indicative of a low degree of reaction / deterioration, DRIs in excess of about 500-600 represent a high to very high (DRI > 1000) degree of ASR. It is important to mention, however, that since the DRI is not a standardized method, values can vary significantly from one petrographer to another.

Table 3. Summary of the petrographic observations on the cores from Alabama (Gibb Graves Bridge)

Sample	DRI	Typical crack width in the concrete (mm)	Extent of ASR	Reactive aggregates in the polished sections
2A-South	1430	Extensive cracking in the cement paste and the aggregate particles; cracks were found to reach 1mm in width (mainly 0.1 to 0.3mm)	Very high degree of ASR	Quartzite and chert
2A-North	1081	Extensive cracking in the cement paste and the aggregate particles; cracks were found to reach 1mm (mainly 0.1 to 0.2mm; several very fine cracks of < 0.05mm in size are filled with compacted ettringite)	High degree of ASR	Quartzite and chert
2B-South	141	No significant cracking in the cement paste (i.e. at the 16x magnification used for the DRI)	No significant ASR	Same type of aggregates as in 2A series but no signs of ASR
2B-North	205	No significant cracking in the cement paste (i.e. at the 16x magnification used for the DRI)	No significant ASR	

4.1 Core 2A-South

Globally, the polished concrete section 2A-South shows several large cracks (up to 1mm in size) that run through the cement paste and the coarse aggregate particles (Figures 1 and B1). The core had

actually to be glued with epoxy to allow the cutting and polishing processes to take place (blue color on the polished section of Figure 1).

The DRI value of **1430** is the highest for the set of cores obtained from the Bibb Graves Bridge (Figures 2 and B1). It is indicative of a very high degree of damage in the concrete. The micrographs in Figure B2 show extensive cracking in the coarse aggregate particles and in the cement paste. As indicated in Figure 2, the highest contributor to the DRI for this core is *Cracks in the cement paste with reaction products* (67% - 964/1430; Figure B2), followed by *Open cracks within the aggregate particles* (12% - 173/1430; e.g. Figure B2-E) and *Cracks with reaction products in the coarse aggregate particles* (7% - 100/1430; Figure B2-B). The coarse aggregates mainly consist of quartzite (Qtz) and chert (Ch) (sometimes partially leached/weathered) particles. Several quartzite aggregate particles show extensive internal cracking and/or grain joints, thus giving a sort of “mosaic” macrotexture (e.g. Figures B2-B and F). Dark reaction rims are observed around some of the above coarse aggregate particles (Figures B2-C and F). The fine aggregate mainly consist of angular to sub-angular quartz grains, with possible fragments of quartzite; it probably has a fairly low modulus of fineness.

Cracks in the cement paste are often filled with whitish/powdery, glassy and/or clear (with a “waxy” luster) secondary reaction products. The examination of concrete fragments under the stereomicroscope (Figure B3) and the scanning electron microscope (SEM) (Figure B4) indicates that the reaction products consist of ettringite (present as clear and “waxy” secondary products under the stereomicroscope as well as in whitish powdery deposits) (Figures B3, B4-B and C; B4-I to K) and alkali-silica gel (Figure B3) that closely co-exist in the deteriorated concrete. Fractured surfaces of the concrete cores reveal a typical arrangement of ASR products (Figures B3-A to C) (i.e. cracks within the aggregate particles and that extend into the cement paste are often filled with alkali-silica gel that gives the typical “mud-crack” texture on such fractured surfaces (Figures B3-G to J)) along with large deposits of ettringite (Figures B3-D to F). Concrete is not air entrained but some voids are filled with ettringite with a clear but “waxy” luster (*ett* on Figures B2-A and D).

4.2 Core 2A-North

Similar to the Core 2A-South, the polished concrete section 2A-North shows several large cracks (up to 1mm in size) that run through the cement paste and the coarse aggregate particles (Figures 1 and B5). The core had also to be glued with epoxy to allow the cutting and polishing processes to take place.

The DRI value of **1081** is the second highest for the set of cores obtained from the Bibb Graves Bridge (Figures 2 and B5). It is indicative of a very high degree of damage in the concrete. The micrographs in Figure B6 show extensive cracking in the coarse aggregate particles and in the cement paste. As indicated in Figures 2 and B5, the highest contributor to the DRI for this core is *Cracks in the cement paste with reaction products* (61% - 664/1081; Figure B6), followed by *Open cracks within the aggregate particles* (11% - 114/1081; e.g. Figure B6-D) and *Cracks in the cement paste (without reaction products)* (10% - 112/1081; Figure B6). The coarse aggregate particles are similar to that in the Core 2A-South and mainly consist of quartzite (Qtz) (possibly some quartzitic sandstone) and chert (Ch) (sometimes partially leached/weathered) particles (Figures B6-A and D). Several quartzite aggregate particles show extensive internal cracking and/or grain joints, thus giving a sort of “mosaic” macrotexture (e.g. Figure B6-F). Dark reaction rims are observed around some of the above coarse aggregate particles (Figures B6-A and B). The fine aggregate mainly consist of angular to sub-angular quartz grains, with possible fragments of quartzite; it probably has a fairly low modulus of fineness.

Similar to Core 2A-South, cracks in the cement paste are often filled with whitish/powdery, glassy and/or clear (with a “waxy” luster) secondary reaction products; some of those cracks are very fine (~0.02-0.03mm). Examination of concrete fragments under the stereomicroscope (Figure B7) indicate that the reaction products consist of ettringite (present as clear and “waxy” secondary products under the stereomicroscope as well as in whitish powdery deposits) (Figure B7-D) and alkali-silica gel (Figures B7-A to C) that co-exist in the deteriorated concrete. Concrete is not air entrained but some voids are filled with ettringite (*ett* in Figures B6-A, B and D).

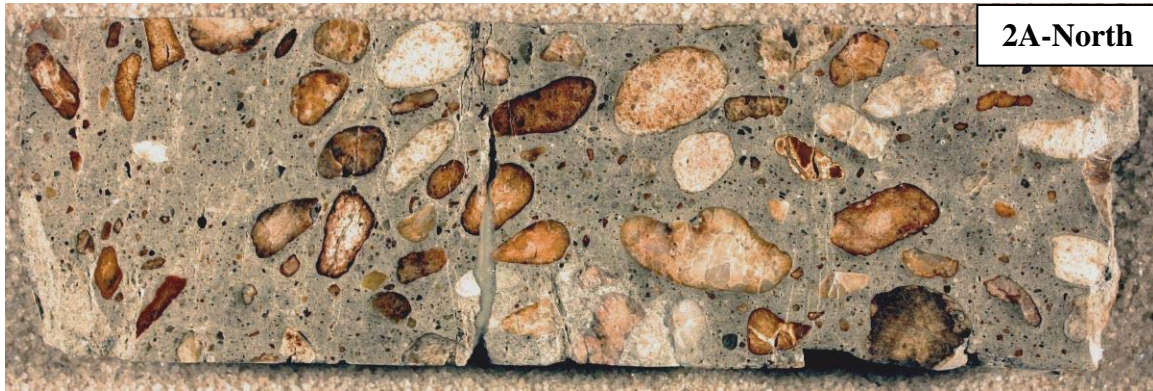
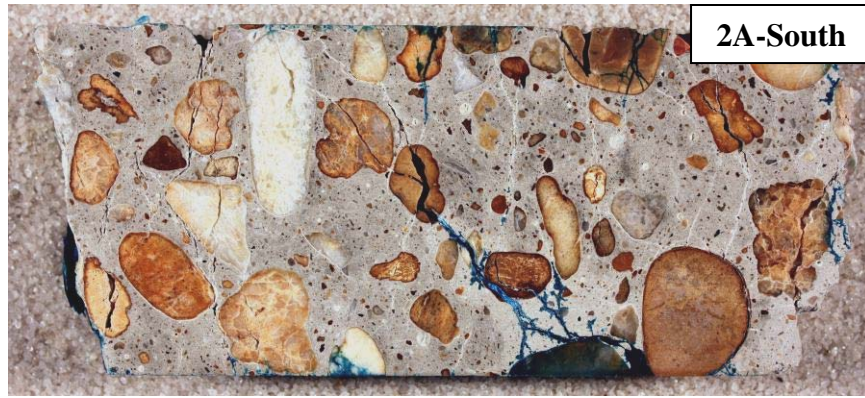


Figure 1. Polished concrete sections from the Gibb Graves Bridge, Wetumpka, Alabama.

Sample	CrCA	OCrCA	Cr+RPCA	CrCP	Cr+RPCP	CAD	RR	RPAV	DRI
2B-North	155	31	1	7	0	0	11	0	205
2B-South	103	31	0	0	0	2	5	1	141
2A-North	78	114	61	112	664	8	14	31	1081
2A-South	96	173	100	29	964	20	10	39	1430

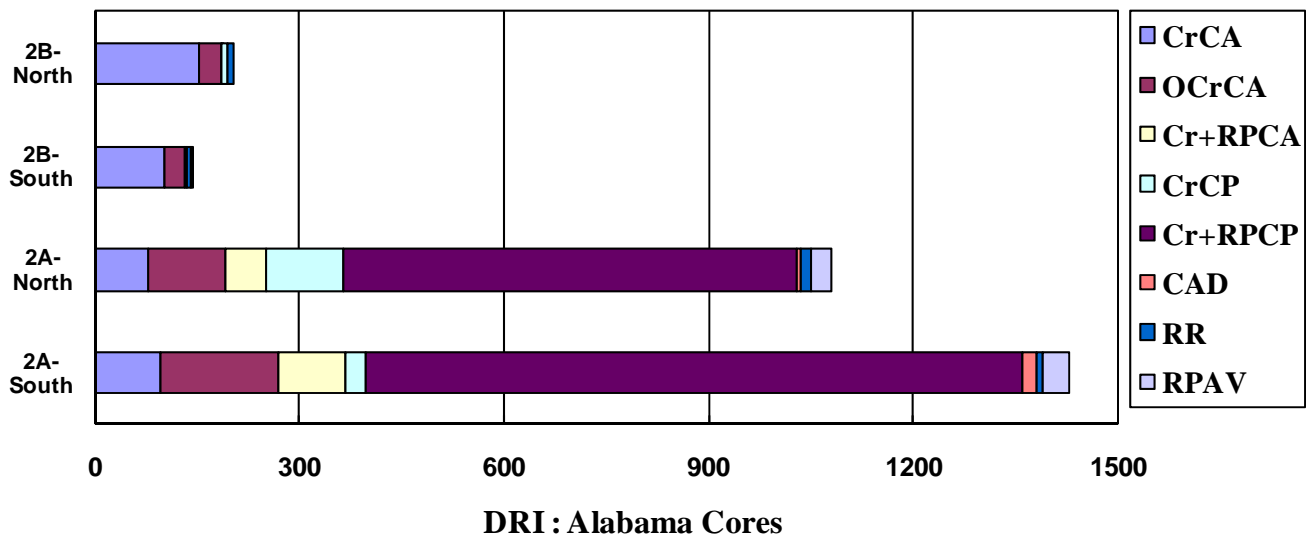


Figure 2. Results of the Damage Rating Index (DRI) for the Alabama cores

4.3 Core 2B-South

The polished concrete section 2B-South shows neither significant cracking nor deterioration (Figures 1 and B8). The DRI value of **141** is the lowest for the set of cores obtained from the Bibb Graves Bridge (Figures 2 and B8). It is indicative of a very low degree of damage in the concrete. As indicated in Figure 2, the highest contributor to the DRI for this core is *Cracks in the aggregate particles (without reaction products)* (73% - 103/141; Figure B9), followed by *Open cracks within the aggregate particles* (22% - 31/141). The coarse aggregate is similar to that of the set of 2A cores and mainly consist of quartzite (Qtz) (also possibly quartzitic sandstone) and chert (Ch) (sometimes partially leached/weathered) particles (Figure B9-D). Several quartzite aggregate particles show extensive internal cracking and/or grain joints, thus giving a sort of “mosaic” macrotexture (e.g. Figures B9-B and C). Dark reaction rims were observed around only a few of the above coarse aggregate particles (~4% of the DRI value). The fine aggregate mainly consist of angular to sub-angular quartz grains, with possible fragments of quartzite; the sand is however coarser than in the cores of the 2A series. No significant cracking, at least at the magnification used for the DRI (16X), was observed in the cement paste. Concrete is not air entrained and the few voids observed are generally empty (no secondary/reaction products).

4.3 Core 2B-North

Similar Core 2B-South, the polished concrete section 2B-North shows neither significant cracking nor deterioration (Figures 1 and B10). The DRI value of **205** is the second lowest for the set of cores obtained from the Bibb Graves Bridge (Figures 2 and B10). It is indicative of a very-low to low degree of damage in the concrete. As indicated in Figure 2, the highest contributor to the DRI for this core is *Cracks in the aggregate particles (without reaction products)* (76% - 155/205; Figure B11), followed by *Open cracks within the aggregate particles* (15% - 31/205). The coarse aggregate is similar to that

of the set of 2A cores and mainly consist of quartzite (Qtz) (also possibly quartzitic sandstone) and chert (Ch) particles (Figure B11). Several quartzite aggregate particles show extensive internal cracking and/or grain joints (e.g. Figures B11-B and E). Dark reaction rims were observed around a few of the above coarse aggregate particles (~5% of the DRI value). The fine aggregate mainly consist of angular to sub-angular quartz grains, with possible fragments of quartzite; the sand is coarser than in the cores of the 2A series. No significant cracking, at least at the magnification used for the DRI (16X) was observed in the cement paste. Concrete is not air entrained but the few voids observed are generally empty (no secondary products).

5 Conclusion - Summary of Findings

Two sets of cores were obtained from the Bibb Graves Bridge (AL Route 111 over Coosa River), Wetumpka, and Alabama. Cores extracted from the arch # 4 (2B-South and 2B-North) are in very good condition and the concrete shows no significant signs of deterioration, as indicated by the low DRI values of 141 and 205. On the other hand, cores extracted from the arch # 5 (2A-South and 2A-North) show several large cracks (up to 1mm in size) that run through the cement paste and the coarse aggregate particles. The DRI values of 1430 and 1081 are indicative of a very high degree of damage in the concrete.

For all concrete core examined (2A and 2B series), the coarse aggregate particles mainly consist of a variety of whitish to brownish quartzite (possibly some quartzitic sandstone) particles, as well as chert particles. The sand is mainly composed of angular to sub-angular quartz and seems to be finer in the set of 2A cores (deteriorated concrete) than for the cores of the 2B series (concrete in good condition).

Concrete cores 2A-South and 2A-North show extensive cracking in the coarse aggregate particles and in the cement paste. Dark reaction rims are observed around several chert and quartzite coarse aggregate particles. Cracks in the cement paste are often filled with whitish/powdery, glassy and/or clear (with a “waxy” luster) secondary reaction products. Further examination of concrete fragments under the stereomicroscope and the SEM confirm the presence of large amounts of ettringite and alkali-silica gel. Thus, the highest contributor to the DRI for those cores correspond to *Cracks in the cement paste with reaction products*, followed by *Open cracks within the aggregate particles* and *Cracks in the aggregate particles with reaction products*.

6 Recommendations

It is first recommended that a detailed structural analysis is performed on the arch affected by ASR. We understand that such an analysis was conducted recently, but that the analysis was based on the assumption that the concrete was undamaged by ASR. The authors of this report are not qualified to comment on the effect of the ASR damage on the structural integrity of the arch.

With regards to suppressing future expansion it is our recommendation that the damaged portions of the arch be treated with a suitable hydrophobic sealer such as a silane. Before application of the silane it is recommend that the concrete surface be cleaned by sand blasting and that the larger cracks be filled with a suitable flexible sealant.

7 References

- Alabama Department of Transportation. 2010. Powerpoint document illustrating the coring and sample preparation processes for the project.
- Dunbar. P.A. and Grattan-Bellew, P.E. 1995. Results of damage rating evaluation of condition of concrete from a number of structures affected by AAR. *In Proceedings of CANMET/ACI International Workshop on AAR in Concrete*, Dartmouth, Nova Scotia, CANMET, Department of Natural Resources Canada, pp. 257-265.
- Grattan-Bellew, P.E. 1992. Comparison of laboratory and field evaluation of alkali-silica reaction in large dams. *In Proceedings of the First International Conference on Concrete Alkali-Aggregate Reactions in Hydroelectric Plants and Dams*, September-October 1992, Fredericton, NB, Canada, 23p.
- Grattan-Bellew, P.E. and Mitchell, L.D. 2006. Quantitative petrographic analysis of concrete – the damage rating index (DRI) method, a review. *Proceedings of Marc-André Bérubé Symposium on Alkali-Aggregate Reaction (AAR) in Concrete*, Montréal (Canada), May 2006, edited by B. Fournier, CANMET-MTL, 45-70.

Appendix A

Coring of the Bibb Graves Bridge
(from ALDOT 2010)

A

INTRODUCTION



View of the Coosa River from the
Bibb Graves Bridge

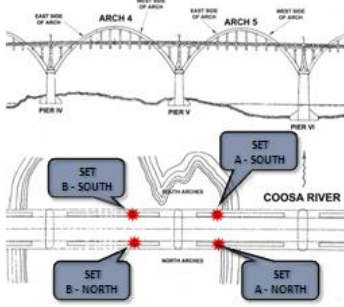


**Bibb Graves Bridge over Coosa River
Wetumpka, Alabama
Constructed in 1930 and 1931
Contains Roquemore Aggregate and
low alkali cement (Average of 0.25
Total per cent Alkali Na₂O)**

BRIDGE LAYOUT
CORE LAYOUT
EXTRACTION PICTURES
CORE SHIPPING

B

CORE LAYOUT



INTRODUCTION
BRIDGE LAYOUT
EXTRACTION PICTURES
CORE SHIPPING

C

CORE SET: A - SOUTH




<table border="1" style="width: 100%; border-collapse: collapse;"> <tr><td>CORE ID:</td><td>1A-S</td></tr> <tr><td>CORE LOCATION:</td><td>South arch #3. West side of arch. Approximately 17' 11" from top of pedestal.</td></tr> <tr><td>CORE REMARKS:</td><td>Full core obtained in two sections on 01/14/2010: Section 1: Approx. 4' 4" Section 2: Approx. 4' 4" No discoloration, if any, from labeling marker.</td></tr> </table>	CORE ID:	1A-S	CORE LOCATION:	South arch #3. West side of arch. Approximately 17' 11" from top of pedestal.	CORE REMARKS:	Full core obtained in two sections on 01/14/2010: Section 1: Approx. 4' 4" Section 2: Approx. 4' 4" No discoloration, if any, from labeling marker.	<table border="1" style="width: 100%; border-collapse: collapse;"> <tr><td>CORE ID:</td><td>2A-S</td></tr> <tr><td>CORE LOCATION:</td><td>South arch #3. West side of arch. Approximately 17' 11" from top of pedestal.</td></tr> <tr><td>CORE REMARKS:</td><td>Full core obtained in three sections on 01/14/2010: Section 1: Approx. 8' Section 2: Approx. 6' 10" Section 3: Approx. 1" No discoloration, if any, from labeling marker.</td></tr> </table>	CORE ID:	2A-S	CORE LOCATION:	South arch #3. West side of arch. Approximately 17' 11" from top of pedestal.	CORE REMARKS:	Full core obtained in three sections on 01/14/2010: Section 1: Approx. 8' Section 2: Approx. 6' 10" Section 3: Approx. 1" No discoloration, if any, from labeling marker.
CORE ID:	1A-S												
CORE LOCATION:	South arch #3. West side of arch. Approximately 17' 11" from top of pedestal.												
CORE REMARKS:	Full core obtained in two sections on 01/14/2010: Section 1: Approx. 4' 4" Section 2: Approx. 4' 4" No discoloration, if any, from labeling marker.												
CORE ID:	2A-S												
CORE LOCATION:	South arch #3. West side of arch. Approximately 17' 11" from top of pedestal.												
CORE REMARKS:	Full core obtained in three sections on 01/14/2010: Section 1: Approx. 8' Section 2: Approx. 6' 10" Section 3: Approx. 1" No discoloration, if any, from labeling marker.												

CORE LAYOUT
NEXT

D

CORE SET: B - SOUTH




<table border="1" style="width: 100%; border-collapse: collapse;"> <tr><td>CORE ID:</td><td>1B-S</td></tr> <tr><td>CORE LOCATION:</td><td>South arch #4. West side of arch. Approximately 2' 6" from top of pedestal.</td></tr> <tr><td>CORE REMARKS:</td><td>Full core obtained in one section on 01/14/2010: Section 1: Approx. 10' 11" No discoloration, if any, from labeling marker.</td></tr> </table>	CORE ID:	1B-S	CORE LOCATION:	South arch #4. West side of arch. Approximately 2' 6" from top of pedestal.	CORE REMARKS:	Full core obtained in one section on 01/14/2010: Section 1: Approx. 10' 11" No discoloration, if any, from labeling marker.	<table border="1" style="width: 100%; border-collapse: collapse;"> <tr><td>CORE ID:</td><td>2B-S</td></tr> <tr><td>CORE LOCATION:</td><td>South arch #4. West side of arch. Approximately 2' 6" from top of pedestal.</td></tr> <tr><td>CORE REMARKS:</td><td>Full core obtained in one section on 01/14/2010: Section 1: Approx. 10" No discoloration, if any, from labeling marker.</td></tr> </table>	CORE ID:	2B-S	CORE LOCATION:	South arch #4. West side of arch. Approximately 2' 6" from top of pedestal.	CORE REMARKS:	Full core obtained in one section on 01/14/2010: Section 1: Approx. 10" No discoloration, if any, from labeling marker.
CORE ID:	1B-S												
CORE LOCATION:	South arch #4. West side of arch. Approximately 2' 6" from top of pedestal.												
CORE REMARKS:	Full core obtained in one section on 01/14/2010: Section 1: Approx. 10' 11" No discoloration, if any, from labeling marker.												
CORE ID:	2B-S												
CORE LOCATION:	South arch #4. West side of arch. Approximately 2' 6" from top of pedestal.												
CORE REMARKS:	Full core obtained in one section on 01/14/2010: Section 1: Approx. 10" No discoloration, if any, from labeling marker.												

PREVIOUS
CORE LAYOUT
NEXT

E

CORE SET: A - NORTH

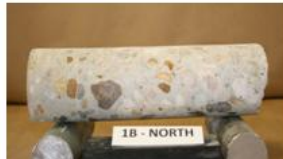



<table border="1" style="width: 100%; border-collapse: collapse;"> <tr><td>CORE ID:</td><td>1A-N</td></tr> <tr><td>CORE LOCATION:</td><td>North arch #3. West side of arch. Approximately 16' 2" from top of pedestal.</td></tr> <tr><td>CORE REMARKS:</td><td>Full core obtained in two sections on 01/14/2010: Section 1: Approx. 5' 9" Section 2: Approx. 2' 10" No discoloration, if any, from labeling marker.</td></tr> </table>	CORE ID:	1A-N	CORE LOCATION:	North arch #3. West side of arch. Approximately 16' 2" from top of pedestal.	CORE REMARKS:	Full core obtained in two sections on 01/14/2010: Section 1: Approx. 5' 9" Section 2: Approx. 2' 10" No discoloration, if any, from labeling marker.	<table border="1" style="width: 100%; border-collapse: collapse;"> <tr><td>CORE ID:</td><td>2A-N</td></tr> <tr><td>CORE LOCATION:</td><td>North arch #3. West side of arch. Approximately 16' 2" from top of pedestal.</td></tr> <tr><td>CORE REMARKS:</td><td>Full core obtained in two sections on 01/14/2010: Section 1: Approx. 4' 11" Section 2: Approx. 2' 4" No discoloration, if any, from labeling marker.</td></tr> </table>	CORE ID:	2A-N	CORE LOCATION:	North arch #3. West side of arch. Approximately 16' 2" from top of pedestal.	CORE REMARKS:	Full core obtained in two sections on 01/14/2010: Section 1: Approx. 4' 11" Section 2: Approx. 2' 4" No discoloration, if any, from labeling marker.
CORE ID:	1A-N												
CORE LOCATION:	North arch #3. West side of arch. Approximately 16' 2" from top of pedestal.												
CORE REMARKS:	Full core obtained in two sections on 01/14/2010: Section 1: Approx. 5' 9" Section 2: Approx. 2' 10" No discoloration, if any, from labeling marker.												
CORE ID:	2A-N												
CORE LOCATION:	North arch #3. West side of arch. Approximately 16' 2" from top of pedestal.												
CORE REMARKS:	Full core obtained in two sections on 01/14/2010: Section 1: Approx. 4' 11" Section 2: Approx. 2' 4" No discoloration, if any, from labeling marker.												

PREVIOUS
CORE LAYOUT
NEXT

F

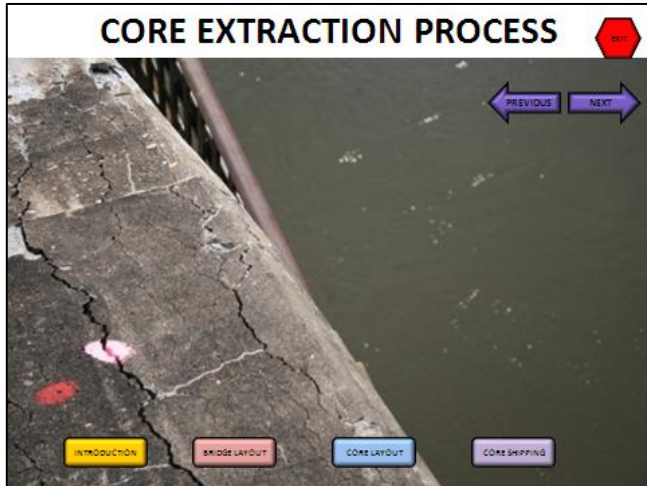
CORE SET: B - NORTH




<table border="1" style="width: 100%; border-collapse: collapse;"> <tr><td>CORE ID:</td><td>1B-N</td></tr> <tr><td>CORE LOCATION:</td><td>North arch #4. West side of arch. Approximately 2' 10" from top of pedestal.</td></tr> <tr><td>CORE REMARKS:</td><td>Full core obtained in one section on 01/14/2010: Section 1: Approx. 11' 4" No discoloration, if any, from labeling marker.</td></tr> </table>	CORE ID:	1B-N	CORE LOCATION:	North arch #4. West side of arch. Approximately 2' 10" from top of pedestal.	CORE REMARKS:	Full core obtained in one section on 01/14/2010: Section 1: Approx. 11' 4" No discoloration, if any, from labeling marker.	<table border="1" style="width: 100%; border-collapse: collapse;"> <tr><td>CORE ID:</td><td>2B-N</td></tr> <tr><td>CORE LOCATION:</td><td>North arch #4. West side of arch. Approximately 2' 10" from top of pedestal.</td></tr> <tr><td>CORE REMARKS:</td><td>Full core obtained in one section on 01/14/2010: Section 1: Approx. 10" No discoloration, if any, from labeling marker.</td></tr> </table>	CORE ID:	2B-N	CORE LOCATION:	North arch #4. West side of arch. Approximately 2' 10" from top of pedestal.	CORE REMARKS:	Full core obtained in one section on 01/14/2010: Section 1: Approx. 10" No discoloration, if any, from labeling marker.
CORE ID:	1B-N												
CORE LOCATION:	North arch #4. West side of arch. Approximately 2' 10" from top of pedestal.												
CORE REMARKS:	Full core obtained in one section on 01/14/2010: Section 1: Approx. 11' 4" No discoloration, if any, from labeling marker.												
CORE ID:	2B-N												
CORE LOCATION:	North arch #4. West side of arch. Approximately 2' 10" from top of pedestal.												
CORE REMARKS:	Full core obtained in one section on 01/14/2010: Section 1: Approx. 10" No discoloration, if any, from labeling marker.												

PREVIOUS
CORE LAYOUT
NEXT

A



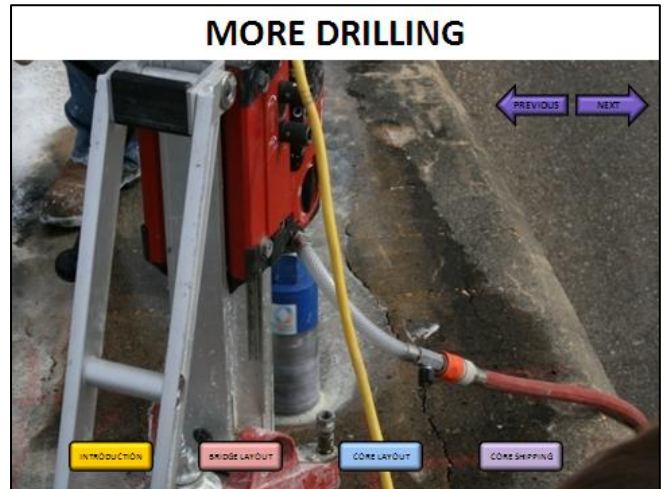
B



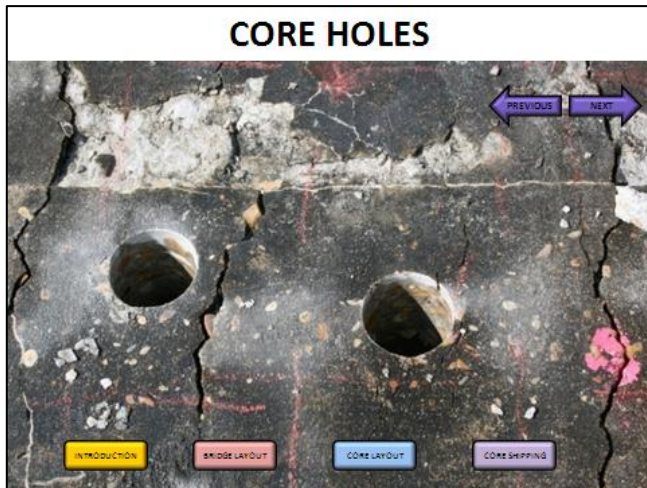
C



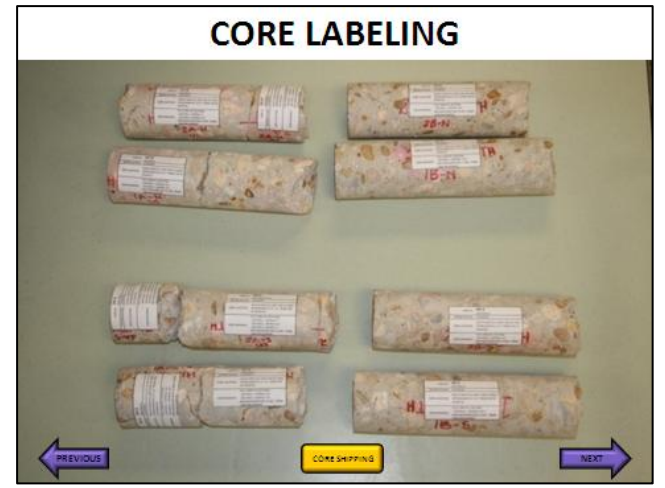
D



E



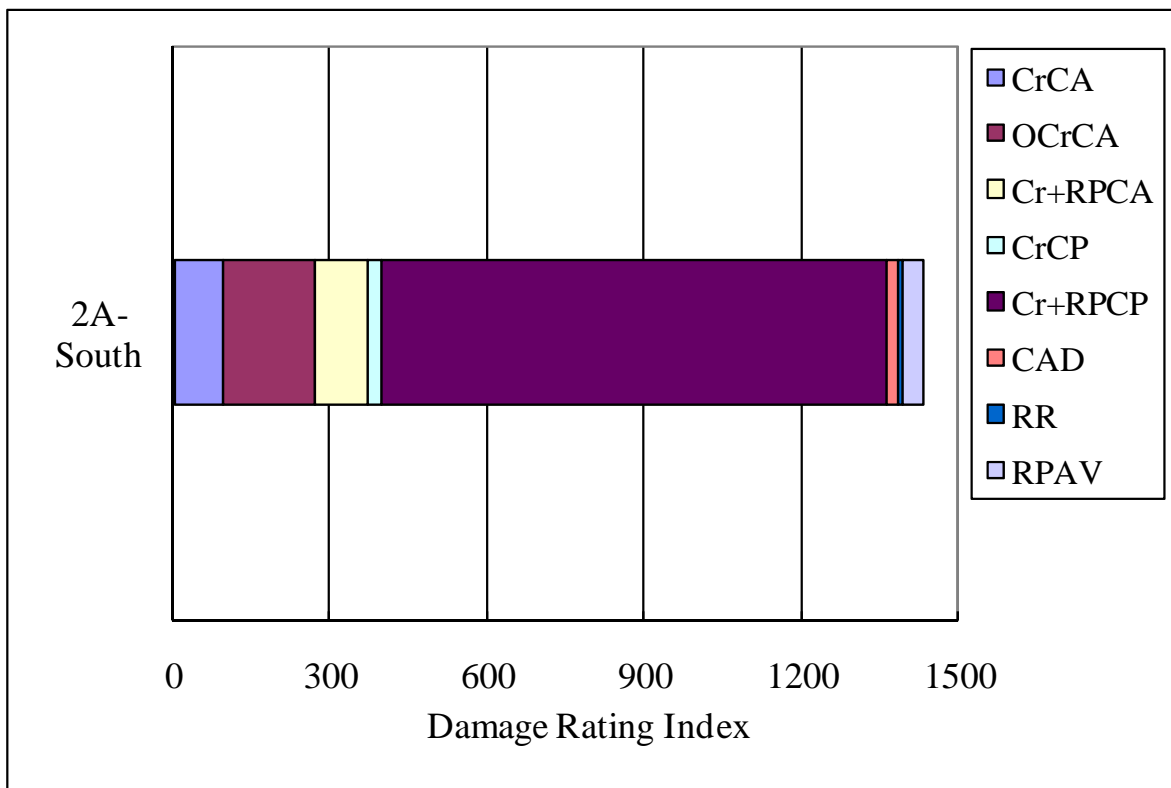
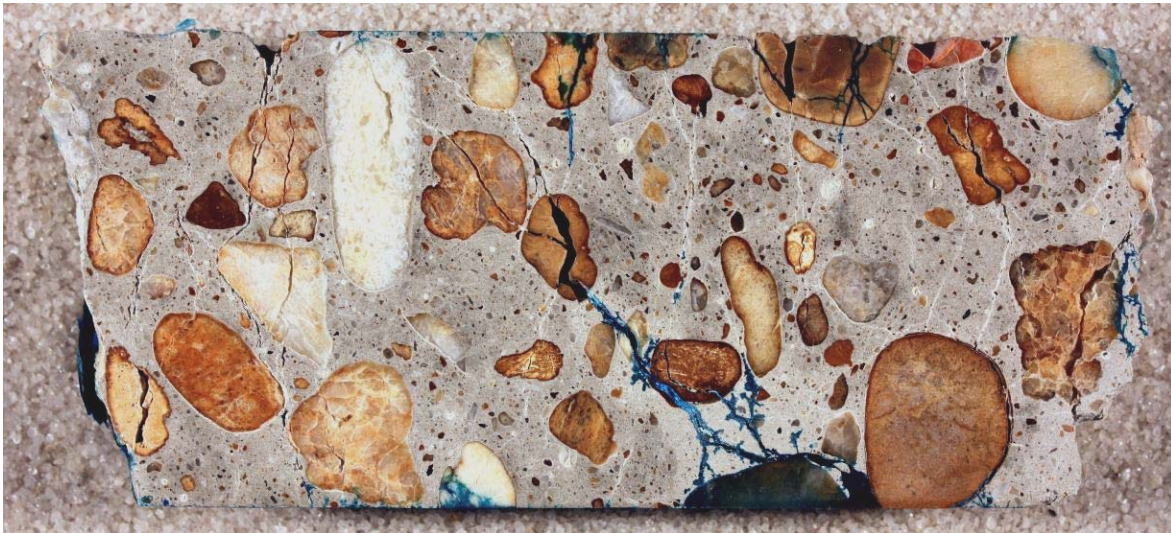
F



Appendix B

Photographs of the polished concrete core sections,
detailed results of the DRI and
micrographs of the petrographic symptoms of deterioration

CORE: 2A-South



Sample	CrCA	OCrCA	Cr+RPCA	CrCP	Cr+RPCP	CAD	RR	RPAV	DRI
2A-South	96	173	100	29	964	20	10	39	1430

Figure B1: Polished core section 2A-South and DRI results

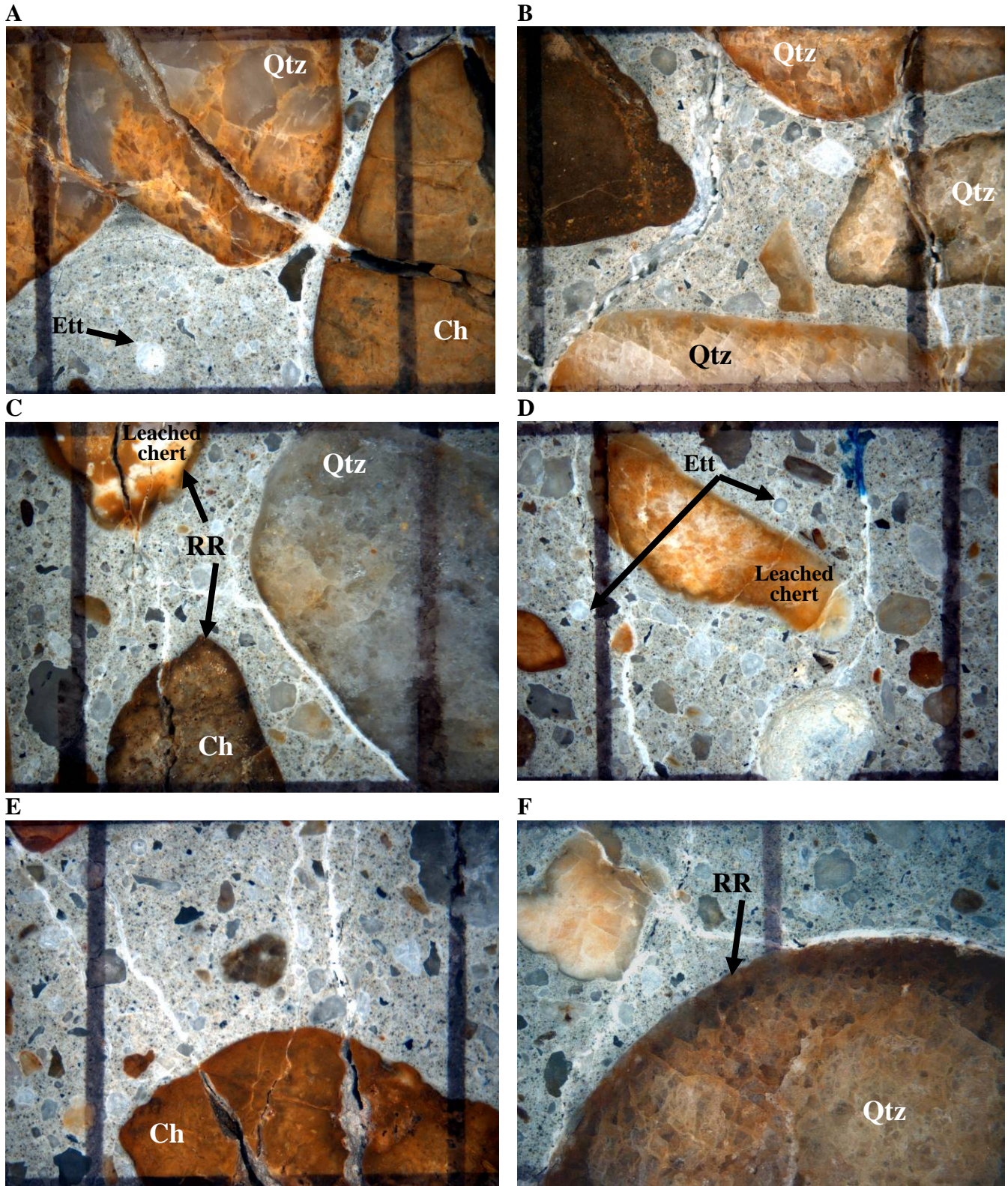


Figure B2: Micrographs of the polished core section 2A-South (distance between vertical lines = 1 cm)
 The micrographs show extensive cracking in the coarse aggregate particles and in the cement paste. The coarse aggregates mainly consist of chert (Ch) (sometimes partially leached/weathered) and quartzite particles (Qtz). Dark reaction rims (RR) are observed around some coarse aggregate particles. Concrete is not air entrained but some air voids are filled with ettringite (ett) (e.g. D). Cracks in the cement paste are often filled by ettringite (whitish and powdery deposits; also clear and waxy in luster) and alkali-silica reaction products, as illustrated in more details in Figure B3.

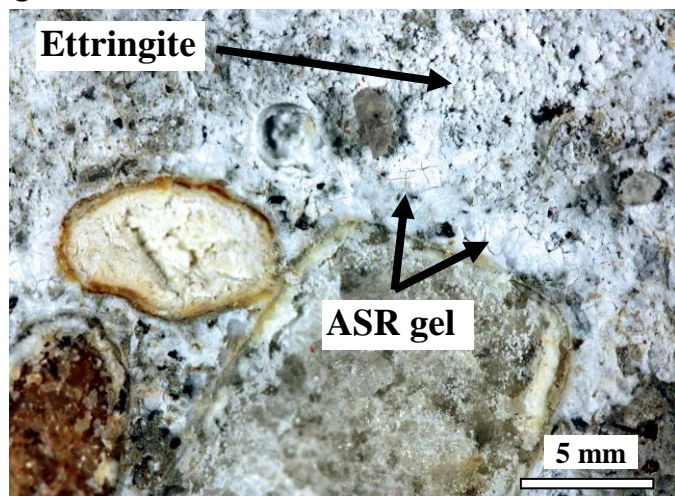
A



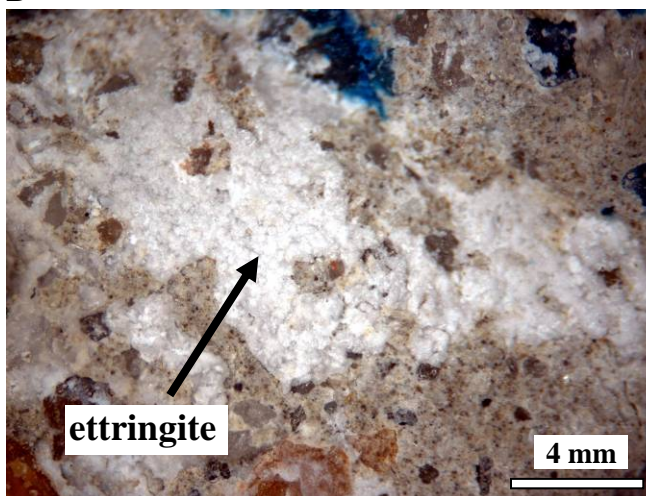
B



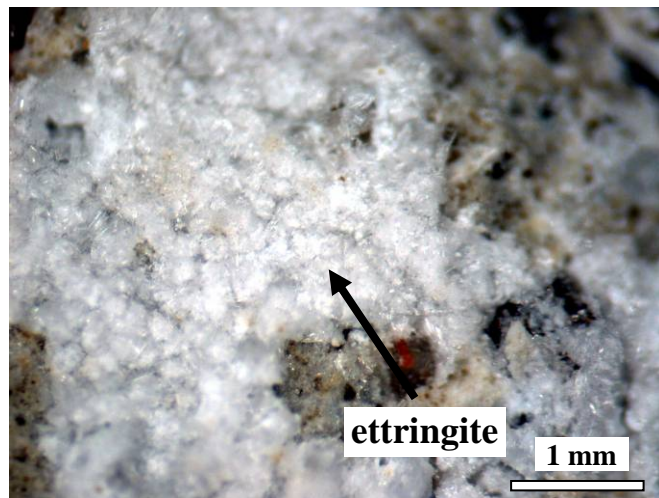
C



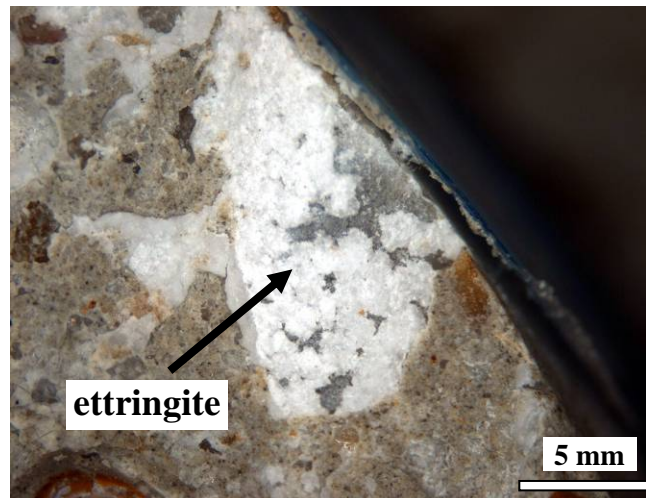
D



E



F



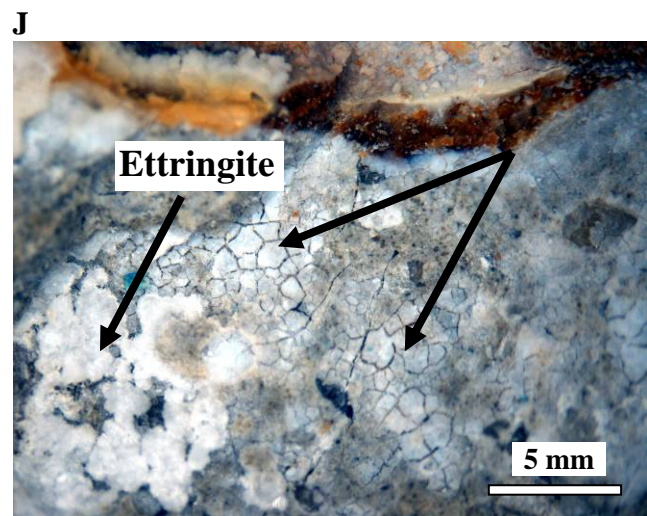
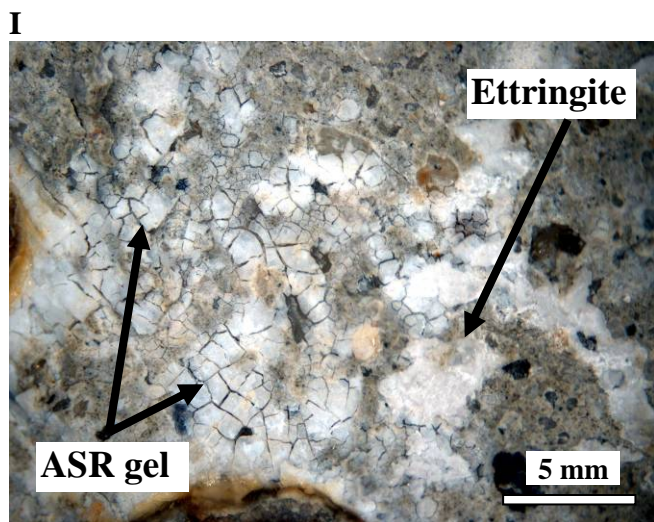
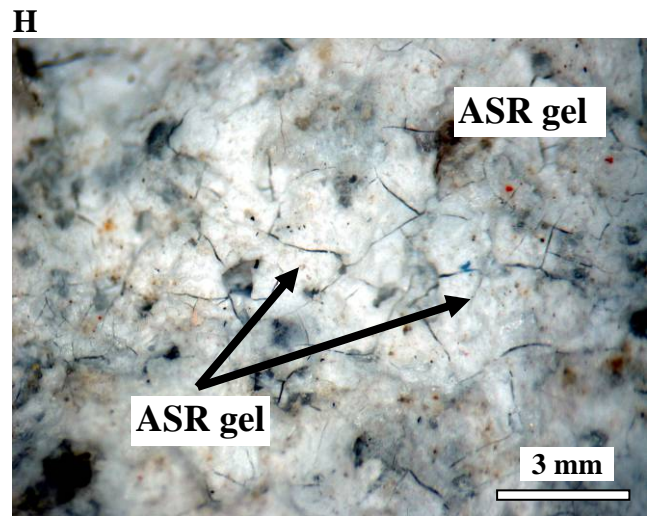
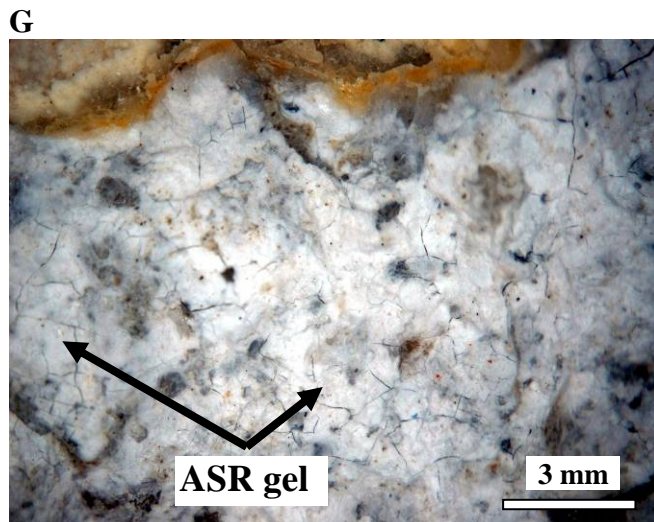


Figure B3: Micrographs of broken surfaces of the core 2A-South, as examined under the stereomicroscope. Figures B3-A and B3-B. Concrete surfaces broken along major cracks in the cement paste (core diameter = 3 inches (75mm)). Figure B3-C. The core broke along large cracks in the cement paste, thus exposing surfaces, both along cracks in the aggregates and the cement paste, largely covered by whitish secondary reaction products. Such products consist of ettringite and ASR gel (18x magnification). Figure B3-D. Whitish (powdery) reaction products (ettringite) covering large areas of the cement paste (20x magnification). Figure B3-E: Magnification (30x) of the reaction products illustrated in B3-D showing the needle-type microtexture of ettringite. Figure B3-F. Deposit of ettringite covering an aggregate particle. The deposit was found at the interface between an aggregate particle and the cement paste (as in Figure B2-C) and caused debonding of the aggregate particle when the concrete was broken for petrographic examination (20x magnification). Figures B3-G and B3-H. Deposits of ASR gel (showing typical “mud-crack” microtexture) covering large areas of the cracked cement paste (25x magnification). Figures B3-I and B3-J. Deposits of ASR gel and ettringite co-existing in the deteriorated concrete sample (18x magnification).

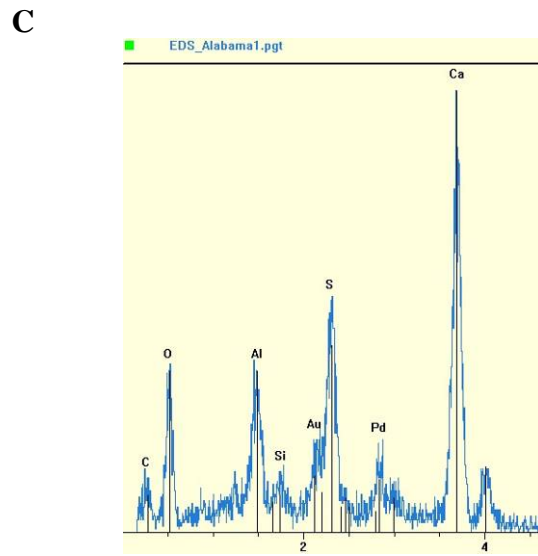
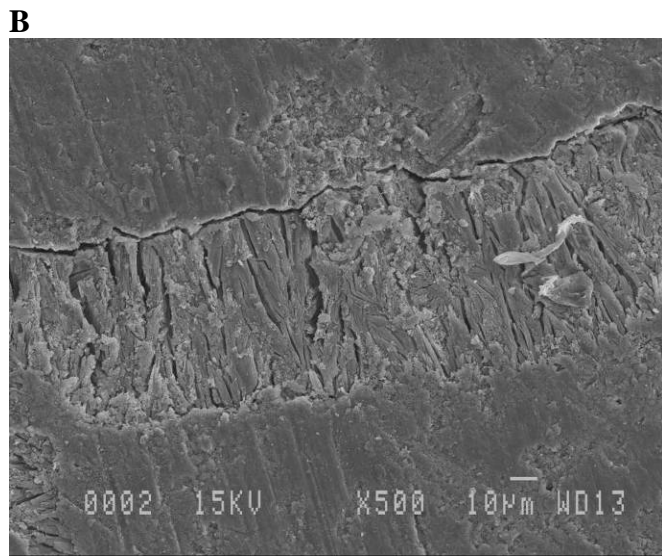
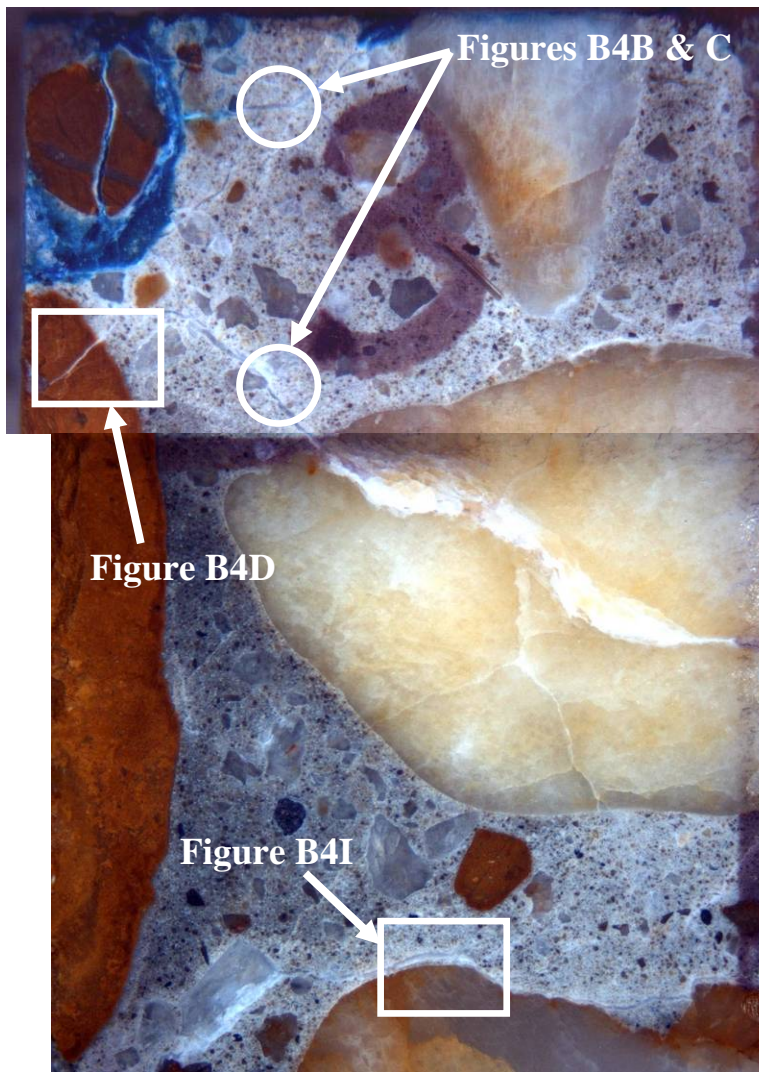
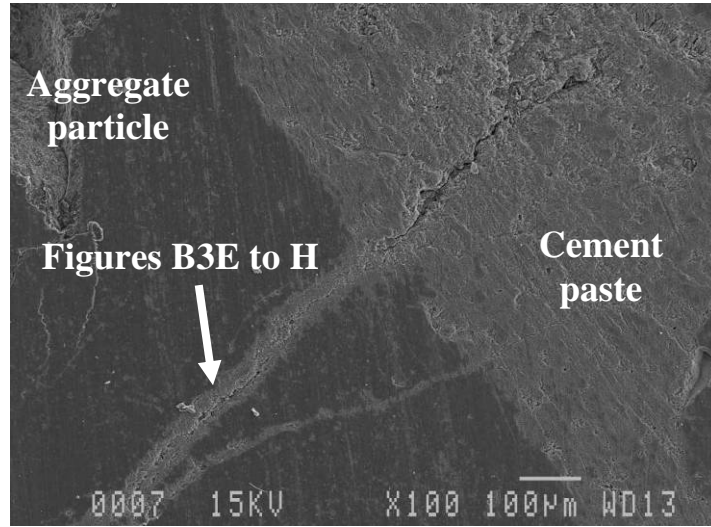
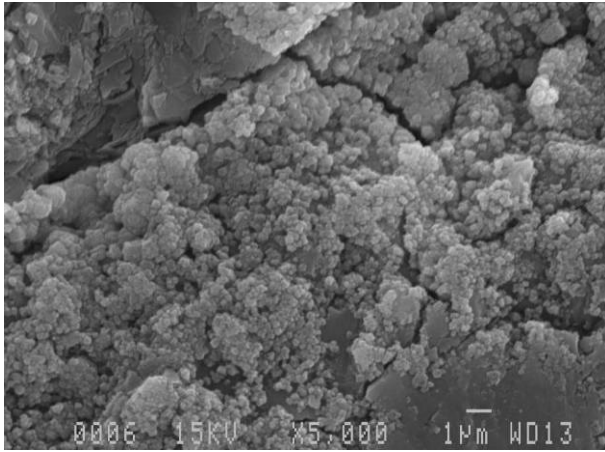


Figure B4: Micrographs of a polished core sample examined under the scanning electron microscope (SEM) (2A-South) (width of micrograph A = 1cm).

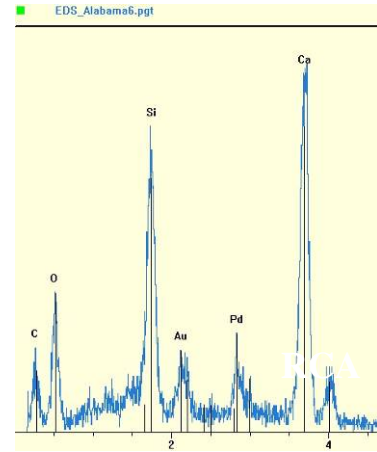
D



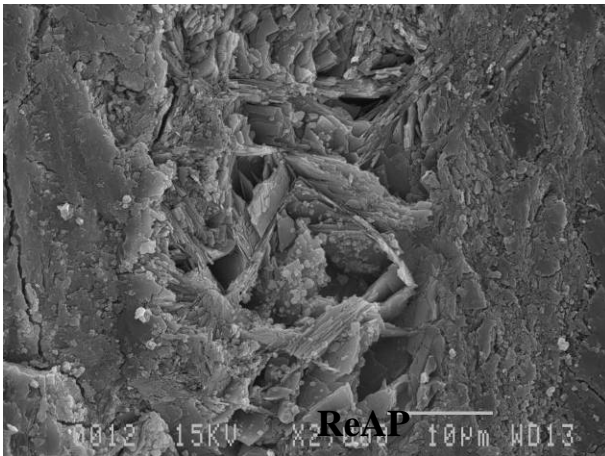
E



F



G



H

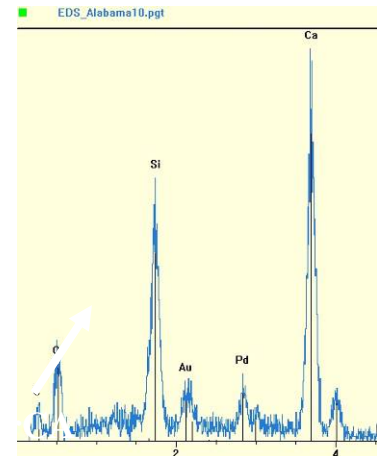


Figure B4 (cont'd)

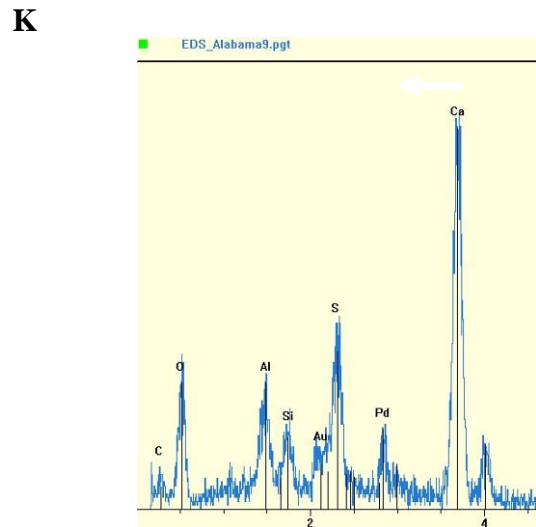
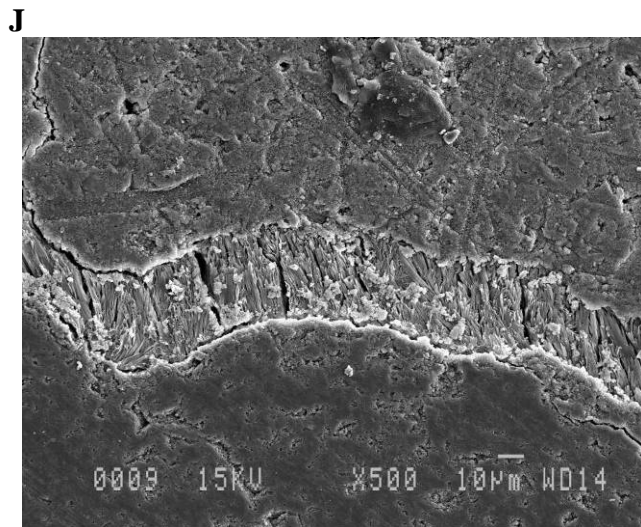
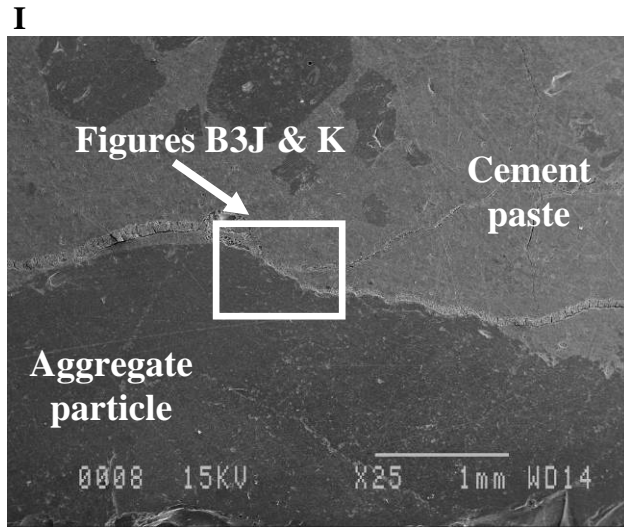
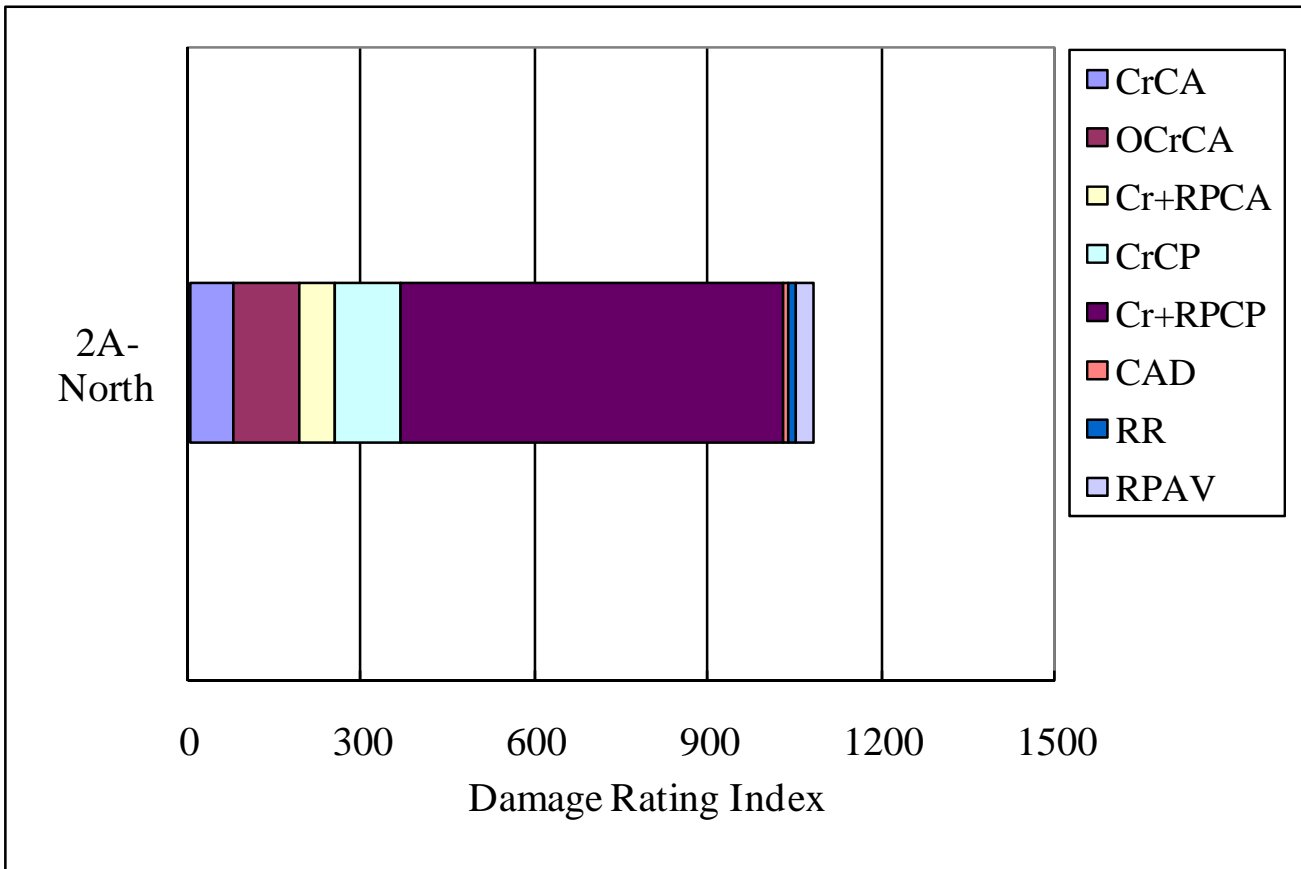


Figure B4 (cont'd): Micrographs of a polished core sample examined under the SEM (2A-South). Figure B4-A. Sample examined under the stereomicroscope. Figure B4-B. Crack filled by compacted ettringite material. Under the stereomicroscope, the ettringite shows a clear but “waxy” luster that differs from that of “glassy” alkali-silica gel. Figure B4-C. Energy dispersive X-Ray analysis of the material (compacted ettringite) filling the crack in micrograph B4-B (typical composition of ettringite including Ca, Al, S; note: the Au and Pd peaks correspond to the conductive metallic deposit at the surface of the sample required for SEM observations). Figure B4-D. Crack extending from the aggregate particle into the cement paste. Figure B4-E. Microtexture of secondary products filling the crack in the aggregate particle illustrated in micrograph B4-D. Figure B4-F. Energy dispersive X-Ray analysis of the material (recrystallized ASR product !?) in micrograph B4-E. Figure B4-G. Microtexture of secondary products filling the crack in the aggregate particle illustrated in micrograph B4-D. Figure B4-H. Energy dispersive X-Ray analysis of the material (recrystallized ASR product !?) in micrograph B4-G. Figure B4-I. Crack in the cement paste above an aggregate particle. Figure B4-J. Microtexture of secondary products filling the crack in the aggregate particle illustrated in micrograph B4-I. Figure B4-K. Energy dispersive X-Ray analysis of the material (compacted ettringite) in micrograph B4-J.

CORE: 2A -North



Sample	CrCA	OCrCA	Cr+RPCA	CrCP	Cr+RPCP	CAD	RR	RPAV	DRI
2A-North	78	114	61	112	664	8	14	31	1081

Figure B5: Polished core section 2A-North and DRI results

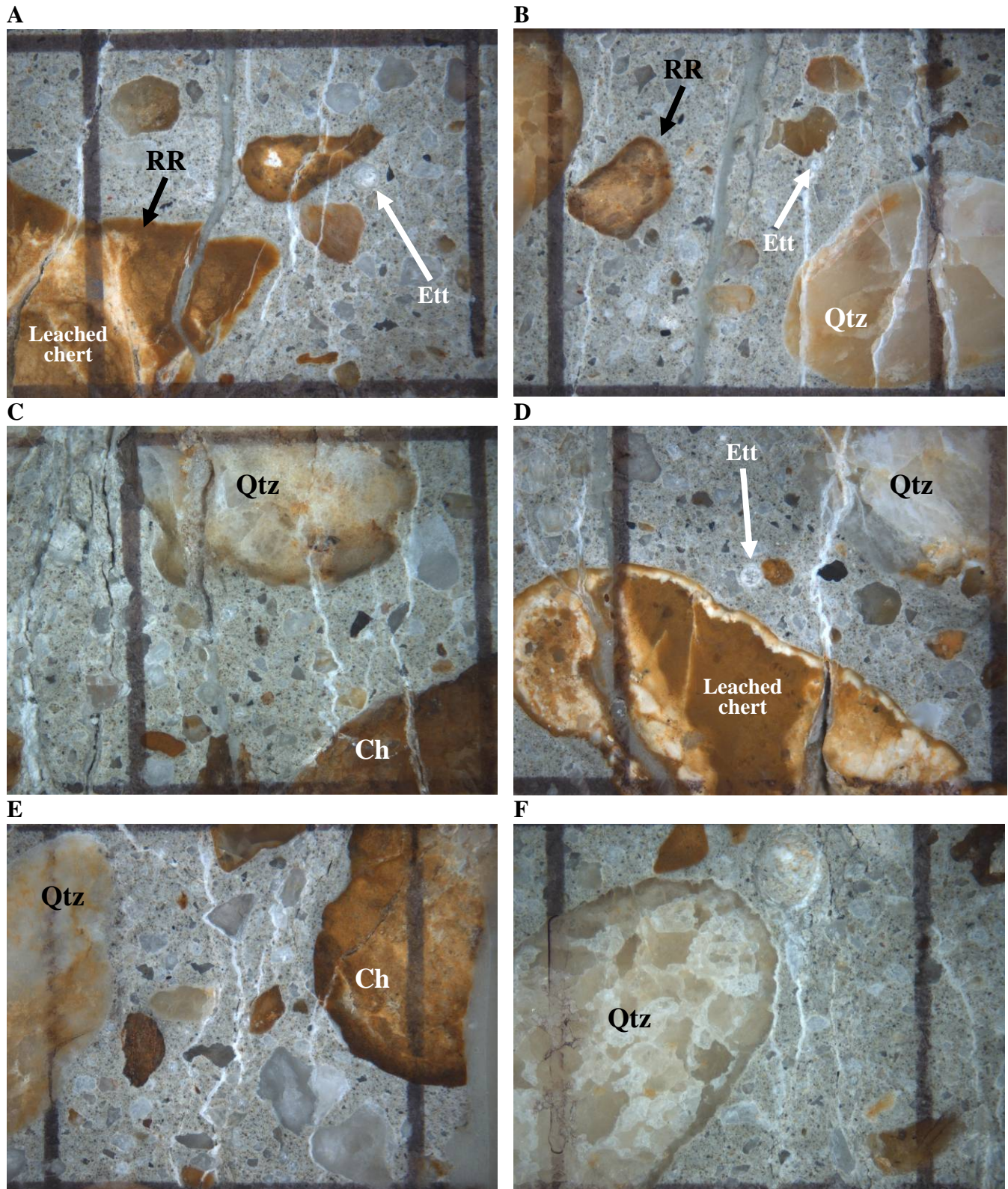


Figure B6: Micrographs of the polished core section 2A-North (distance between vertical lines = 1 cm). The micrographs show extensive cracking in the coarse aggregate particles and in the cement paste. The coarse aggregates mainly consist of chert (Ch)(sometimes partially leached/weathered) and quartzite particles (Qtz). Dark rims (RR) are observed around some coarse aggregate particles. Concrete is not air entrained but some air voids are filled with ettringite (ett) (e.g. B6-A, B6-B and B6-D). Cracks in the cement paste are often filled by ettringite (whitish and powdery deposits; also clear and waxy in luster) and alkali-silica reaction products, as illustrated in more details in Figure B7.

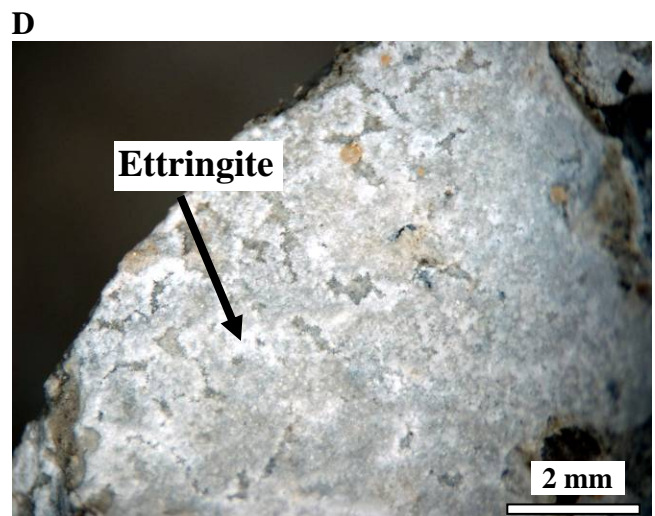
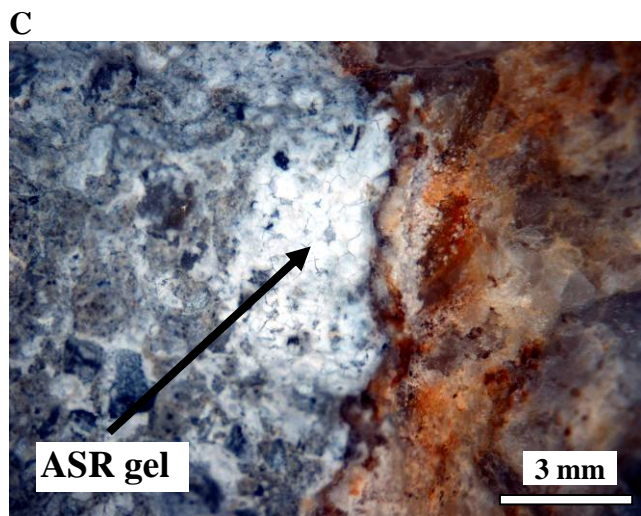
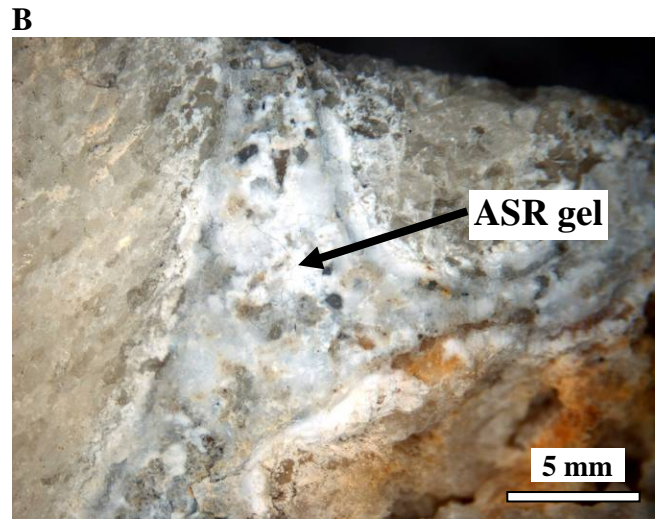
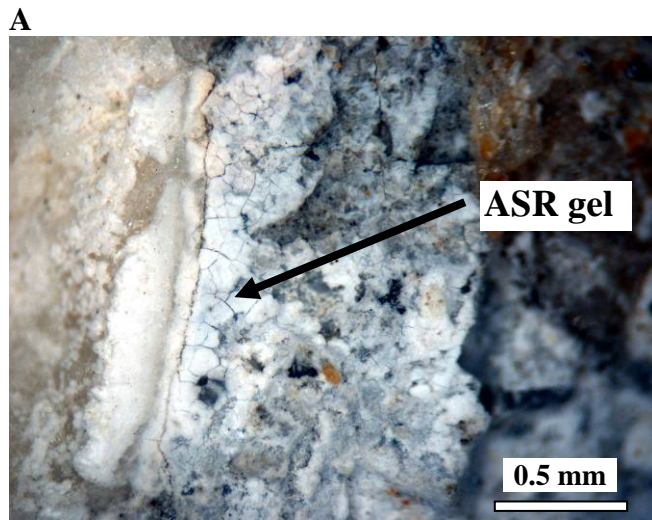
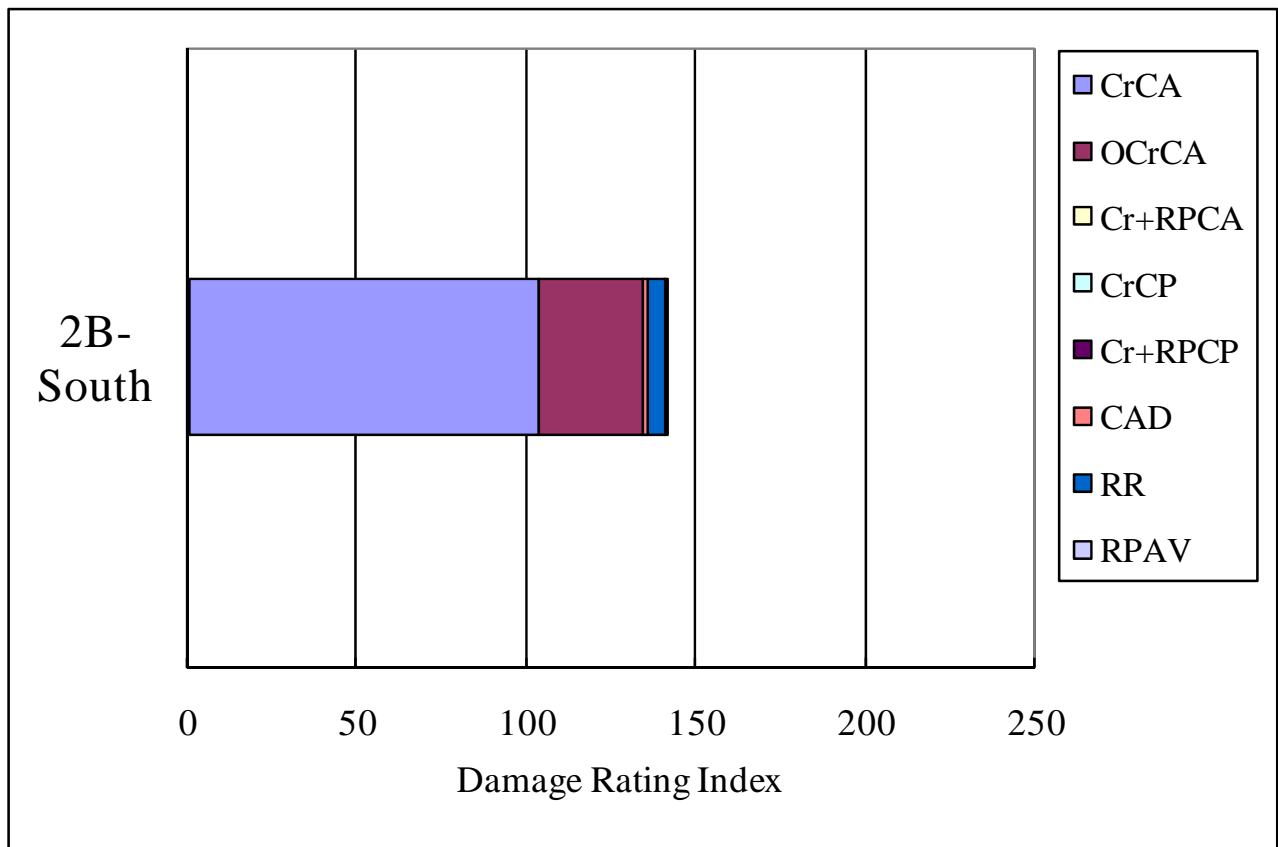


Figure B7: Micrographs of broken surfaces of the core 2A-North, as examined under the stereomicroscope. Figure B7-A to B7-C. Deposits of ASR gel (showing typical “mud-crack” microtexture) covering large areas of the cracked cement paste between aggregate particles. Figure B7-D. Deposit of ettringite in the mold of a debonded aggregate particle. The deposit was found at the interface between the aggregate particle and the cement paste (as in Figure B2-C) and caused debonding of the aggregate particle when the concrete was broken for petrographic examination.

CORE: 2B-South



Sample	CrCA	OCrCA	Cr+RPCA	CrCP	Cr+RPCP	CAD	RR	RPAV	DRI
2B-South	103	31	0	0	0	2	5	1	141

Figure B8: Polished 2B-South core section and DRI results

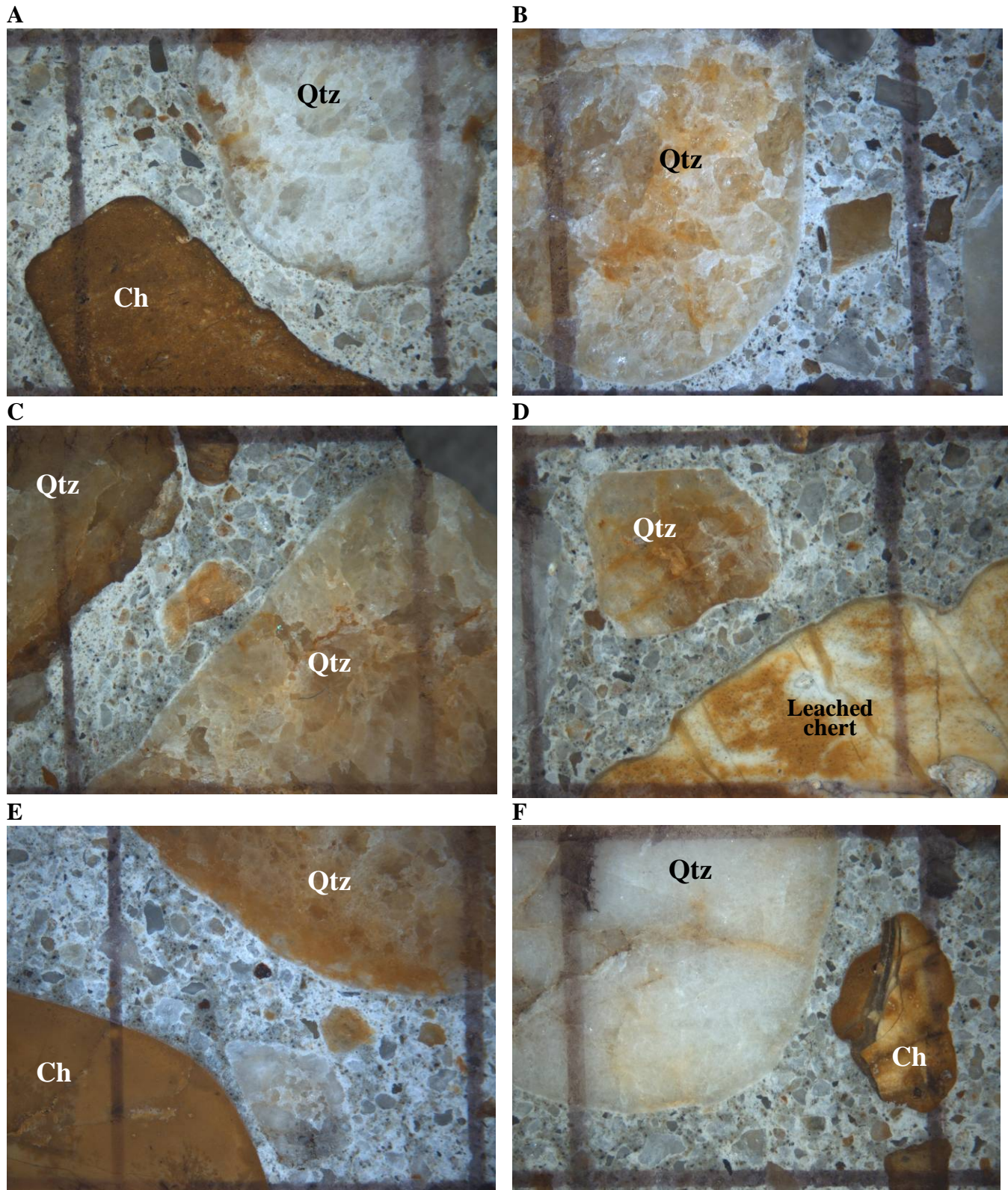
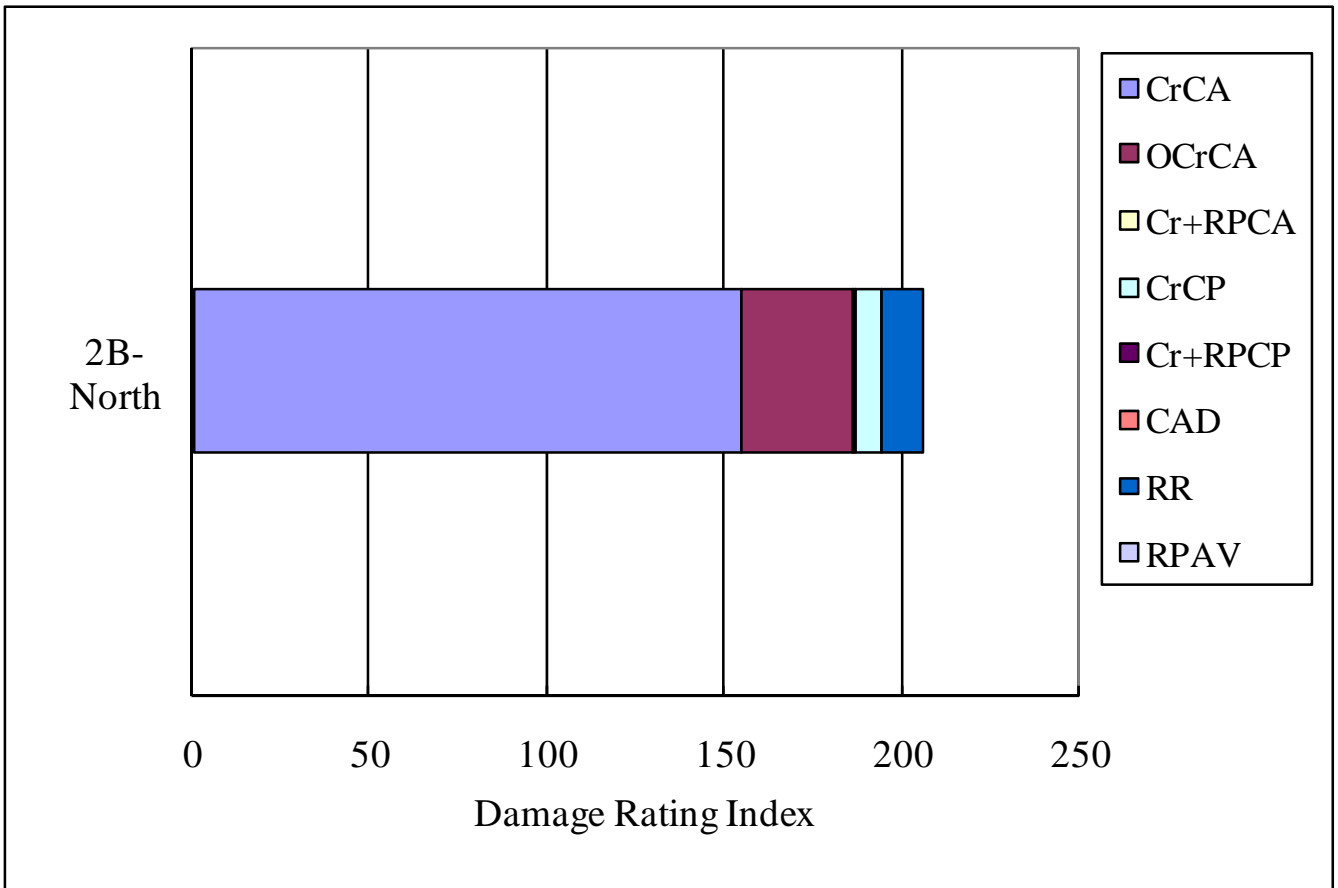


Figure B9: Micrographs of the polished core section 2B-South (distance between vertical lines = 1 cm). The micrographs show coarse aggregate particles that mainly consist of chert (Ch)(sometimes partially leached/weathered) and quartzite particles (Qtz). Very limited cracking is noticed in the cement paste.

CORE: 2B-North



Sample	CrCA	OCrCA	Cr+RPCA	CrCP	Cr+RPCP	CAD	RR	RPAV	DRI
2B-North	155	31	1	7	0	0	11	0	205

Figure B10: Polished 2B-North core section and DRI results

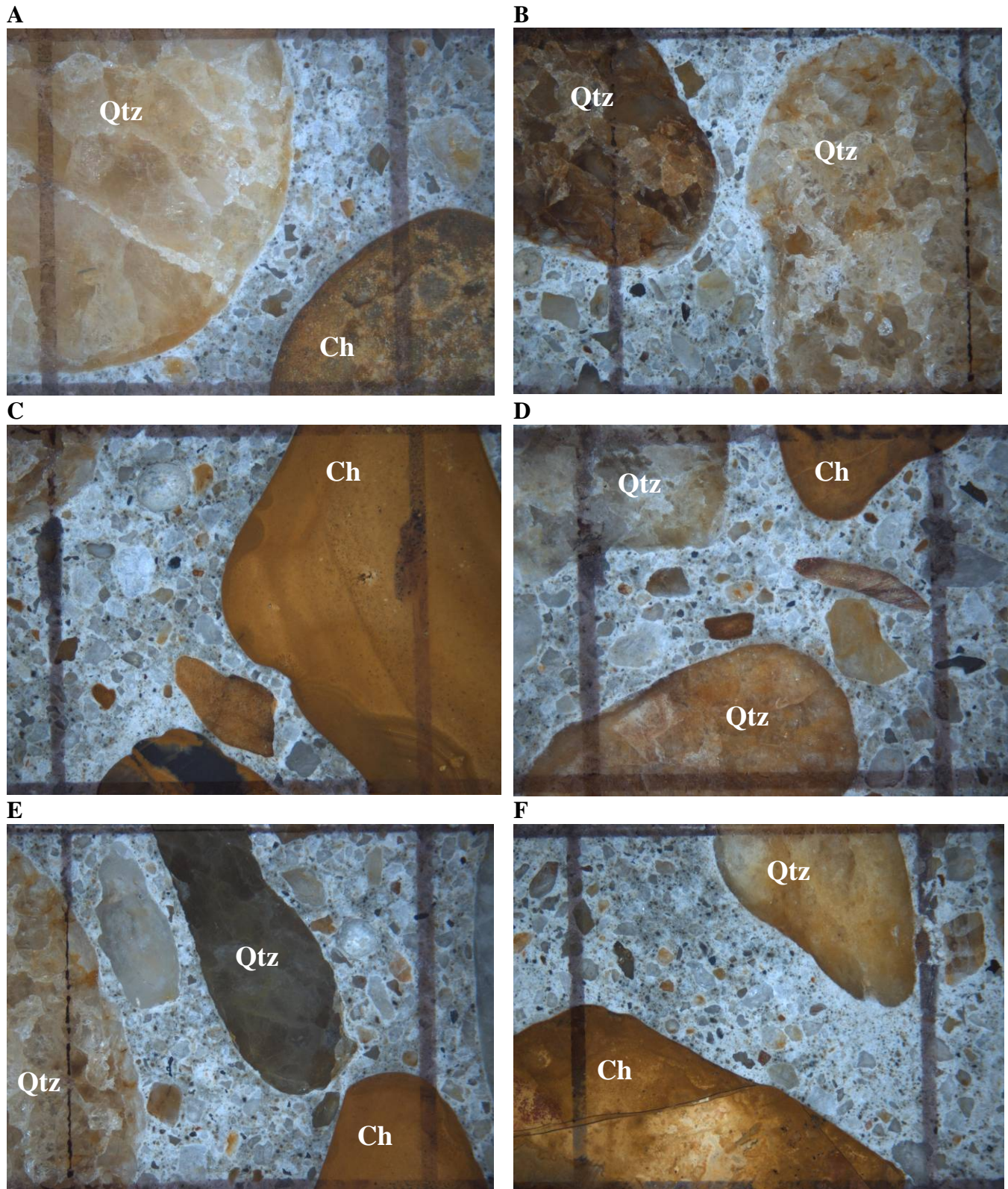


Figure B11: Micrographs of the polished core section 2B-North (distance between vertical lines = 1 cm).The micrographs show coarse aggregate particles that mainly consist of chert (Ch)(sometimes partially leached/weathered) and quartzite particles (Qtz). Very limited cracking is noticed in the cement paste.